Inertial Filtration of Lunar Dust in Lunar Gravity

A Thesis

Submitted in partial satisfaction

For

the Senior Thesis Program in Physics.

By

Emily Sorensen 2008

Carthage College

Kenosha, Wisconsin

April 28, 2008

Examining Committee

_____

_____

_____

Table of Contents

1.0 Experiment Background

1.1 Introduction and Historical Background

The lunar regolith is a layer of unconsolidated material covering the lunar surface to depths of several meters. The regolith material is formed through micrometeorite impacts on the surface of the moon. While the composition of the regolith varies across the lunar surface, the primary constituent of the regolith near the surface of the moon is a fine powdery dust of metallic oxides and silicates. Distribution of particle sizes in the dust ranges from submicron particles to particles in the 25-50 micron range [1].

This dust has been identified as a significant hazard to lunar missions due to its presumed human toxicity [2]. During the Apollo missions, lunar dust was found to adhere to surfaces within the lunar landing module due to the sharp, jagged edges of the dust particles, and because of its electrostatic charge. *In situ*, ultraviolet rays from the sun provide enough energy to remove electrons from the top layers of the regolith, providing a positive charge to the dust [3]. The smaller dust particles have a larger ratio of surface area to volume compared to the larger particles, and therefore a larger surface charge to mass ratio which makes the smaller dust particles even more potentially hazardous [4].

After each moonwalk (EVA) during the Apollo missions, astronauts would inadvertently bring some of the lunar dust on their suits into the Lander. In the instance of Apollo 17 astronaut, Harrison Schmitt, the inhalation of lunar dust caused illness. He reported that the illness came on shortly after he took off his helmet [5]. The cartilage plates in the walls of the nasal chambers can become swollen due to the dust, and clinical trials on mice suggest that respiratory infections can also arise from dust inhalation [6]. After Schmitt's second and third EVA, the illness reappeared but not as severely as it had

the first time. In other cases, several astronauts reported respiratory or eye irritation from the dust.

For the proposed experiment, we will be using a cyclone filter. Cyclone filters are commonly used for dust collection in vacuum cleaners. Cyclones take in dirty air though an inlet. The air then swirls within the cyclone due to its cylindrical shape. As the air continues to flow, it moves in a downward spiral as the diameter of the cyclone decreases. The heavier dust particles pushed against the wall of the cyclone then leave the air stream and fall into a dust collection cup. The airflow then begins to move up through the center of the cyclone taking along with it the smaller dust particles, which are light enough to move up with the airflow. The cyclone that will be used in this experiment will be described in greater detail in Section 7.0 [7].

1.2 Hazards of Lunar Dust

The primary health hazard of lunar dust is associated with the smaller particles that can penetrate and stick to the lung tissue [1]. This so-called "respirable dust" consists of particles with diameters of only a few microns or less. The respirable fraction of lunar dust contains particles of iron oxide that range from 10 – 20 nanometers in diameter [2]. The dust particles of 'nanophase' iron are so small that if inhaled, they can pass from the lungs to the blood stream [1]. Once the 'nanophase' iron is in the blood stream it can bind to hemoglobin molecules that carry oxygen throughout the body. If this were to happen, the body could react in the same way it would if it was exposed to carbon monoxide. However, it is not yet known how much of the 'nanophase' iron is needed for this to happen [2].

Another possible side effect from exposure to lunar dust is silicosis, a disease that killed hundreds of miners from the Hawk's Nest Tunnel during the Great Depression. Silicosis causes lumps and scar tissue on the lungs. It is caused from the inhalation of silica [8]. When the dust is inhaled, it can attach itself into the alveolar sac and ducts where oxygen and carbon dioxide are exchanged. Once the dust reaches this part of the body, it cannot easily be removed with coughing or mucus production. The white blood cells, which would normally carry the particles away in the blood stream, die when they reach the sharp edges of the dust grains. In severe conditions of silicosis, the lungs can fill with proteins from the blood, and the person will slowly suffocate [1].

Apollo astronauts did not experience such severe symptoms, because the time spent on the lunar surface was very short. However, before astronauts return to the lunar surface for extended periods of time, a mechanism for lunar dust mitigation will need to be in place to prevent possible illnesses, since approximately 1–3 percent of the soil is potentially hazardous [9].

1.3 Previous Work

A cyclone filtration system for lunar dust simulants has not been tested on any previous flights on the C-9B aircraft.

2.0 Experiment Description

2.1 Overview and Scientific Goals

Our experiment was designed to assess the efficacy and efficiency of an inertial air filtration system for future lunar habitats. While inertial separation technology

utilizing an air cyclone is well-characterized for filtration applications on Earth, the extent to which reduced gravity affects the efficiency of course particulate filtration in a cyclone is unknown. In particular, cyclone filtration units are designed to meet minimal standards of efficiency characterized by the smallest particle diameter that can be filtered at the 50% level. This *d50* measure is a function of cyclone geometry, air-flow rate, and the molecular structure of the dust particles. Predictive relationships for *d50* as a function of these properties are well-established, but are largely empirical [10].

In our experiment, we characterized a cyclone filtration system on Earth with a lunar dust simulant, which established efficiency measures such as *d50* under 1-g conditions. The same experiments were performed under reduced gravity conditions of 1/6 and 1/3 g conditions, facilitating a comparison of microgravity results and 1-g results. The comparison of flight data and 1-g data directly addresses the role of gravity in inertial filtration systems, which will help validate models and designs of proposed habitat filtration systems.

2.1.1 Conventional Air Filtration Process

A conventional method for the filtration of particulate matter from an airstream is to extract larger particulate matter from the air-flow using an inertial separator. Air flow out of the inertial separator nominally contains only smaller particulate matter which can be more efficiently handled with a conventional HEPA filter (Sec. 3.1.1). The advantage of this method is that the inertial separator is a simple device with no moving parts or filter surfaces to clean.

The separator, or cyclone, shown in Figure [2.1.1], accepts dirty air through an inlet on the side, and due to the conical shape of the cyclone body, induces the air to

move tangentially to the inner surface of the cyclone. The air is spun in a helix of decreasing diameter down the axis of the cyclone. Heavier particulate matter is centrifugally trapped by the walls of the cyclone where it leaves the air stream and migrates to a collection cup at the bottom of the cyclone. The rotating air is exhausted through an axial outlet at the top of the cyclone where it can be processed further with traditional filter media to remove the remaining particulate matter.

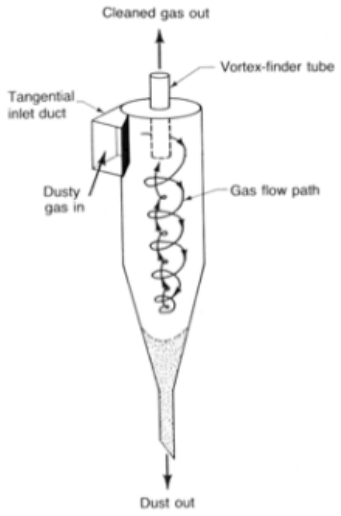

Figure [2.1.1]: Schematic of Cyclone Separator

2.2 Experiment Design

A schematic consisting of the primary components in the experiment is shown in Figure [2.2.1]. Each component in the figure is described in detail in a subsequent section.

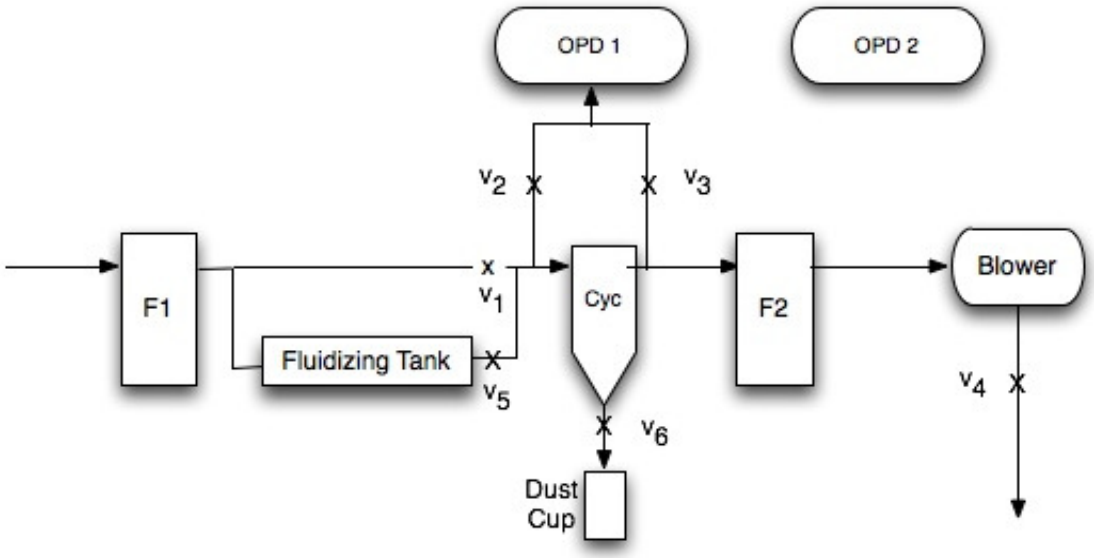

Figure [2.2.1]: Schematic of Experimental Apparatus. Airflow is indicated by arrow direction.

The experiment was conducted with an air-flow created by a blower. Ambient air was induced to flow through the HEPA filter, F1. This step removed any impurities initially in the air. The purified air was then moved to a fluidizing chamber in which the dust simulant was introduced into the air stream and mixed with clean air via valve V1. Valve V1 was an airflow valve that was used to ensure that the dust concentration in the air was within operating range of the optical particle detectors (OPD1 and OPD3), and was consistent from one run to the next.

OPD1 and OPD3 recorded the particle counts in six different bin sizes from submicron to 15 micron particle diameters. Data from OPD1 and OPD3 was then transferred to a laptop computer attached to OPD1 and OPD3 via an RS-232 cable. Valves V2 and V3 allowed the operator to sample particle loading both before and after the cyclone stage. Initially, V2 was open all the way and V3 was opened to a predetermined spot. Airflow past the cyclone consisted largely of unfiltered, small

particulate dust that was trapped by F2. F2 was a HEPA filter, identical to F1. The clean airflow past F2 passed through the blower which was valved by V4 to allow flow rate adjustments. Valve V5 permitted the dust flow to be rapidly attenuated in the unlikely event of a leak during testing or operation and valve V6 prevented dust from leaving the dust collection cup while not in use.

2.3 Flow Rates, Pressure Drops, and Filtration Efficiencies

The blower was capable of generating a flow rate of 15 cfm (this flow-rate was selected to optimize operation of the cyclone unit) under a back pressure of roughly 1 psi. The blower would automatically shutdown if a back pressure greater than 1 psi existed at the inlet. Therefore the net pressure drop across the circuit in Figure [2.2.1] was restricted to 1 psi or less. This condition dictated the choice of tube diameters, effective HEPA filter area, and cyclone geometry. Filters F1 and F2 introduced a few tenths of a psi at 15 cfm. Under nominal particle loading, the cyclone operated with a pressure drop of 0.3 psi at 15 cfm. The fluidizing chamber described in the next section may have introduced a more significant pressure drop, but this drop was mitigated by the valve V1. We expected that the total pressure drop across the circuit would be dominated by the filters F1 and F2, and will be less than 1 psi.

Filtration efficiency is a function of particle diameter, cyclone geometry, and the kinematic properties of air. Shepherd and Lapple [7] derived a standard model for the relationship between cyclone design parameters and efficiency measures, such as *d50*, which was described in section 2.1. The derivation will not be repeated here, but its central result can be expressed in terms of *d50* as

$$d_{50} = \left[\frac{9\mu W}{2\pi N V_i (\rho_p - \rho_g)} \right]^{1/2}. \qquad \text{(Eq. 1)}$$

Here, μ is the kinematic viscosity of air, W is the inlet diameter, ρ_p is the specific gravity of the particulate matter, and ρ_g is the density of air. The velocity at the air inlet, V_i can be calculated from the flow rate Q and the inlet diameter, W: $Q = V_i (\pi W^2/4)$. The effective number of turns experienced by the air inside the cyclone is a function of the two characteristic lengths L_{cone} and $L_{cylinder}$ of the cyclone:

$$N = \frac{1}{W}\left(L_{cylinder} + \frac{L_{cone}}{2} \right). \qquad \text{(Eq. 2)}$$

The relevant dimensional and kinematic values for a calculation of *d50* are compiled in Table [2.3.1].

Cyclone Geometry (inch)	
W	1.00
$L_{cylinder}$	4.15
L_{cone}	5.53
Kinematic Properties	
μ (kg m/s)	1.75×10^{-5}
ρ_p (kg/m^3)	2900
ρ_g (kg/m^3)	1.30

Table [2.3.1]: Parameters used in the calculation of Cyclone Efficiency

Based on this model, we calculated values of *d50* over the range of accessible flow rates *Q*. This data displayed in Figure [2.3.1] suggests that we can expect a 50% filtration efficiency between 1.1 and 1.8 microns over a flow rate range of 10-30 cfm [10].

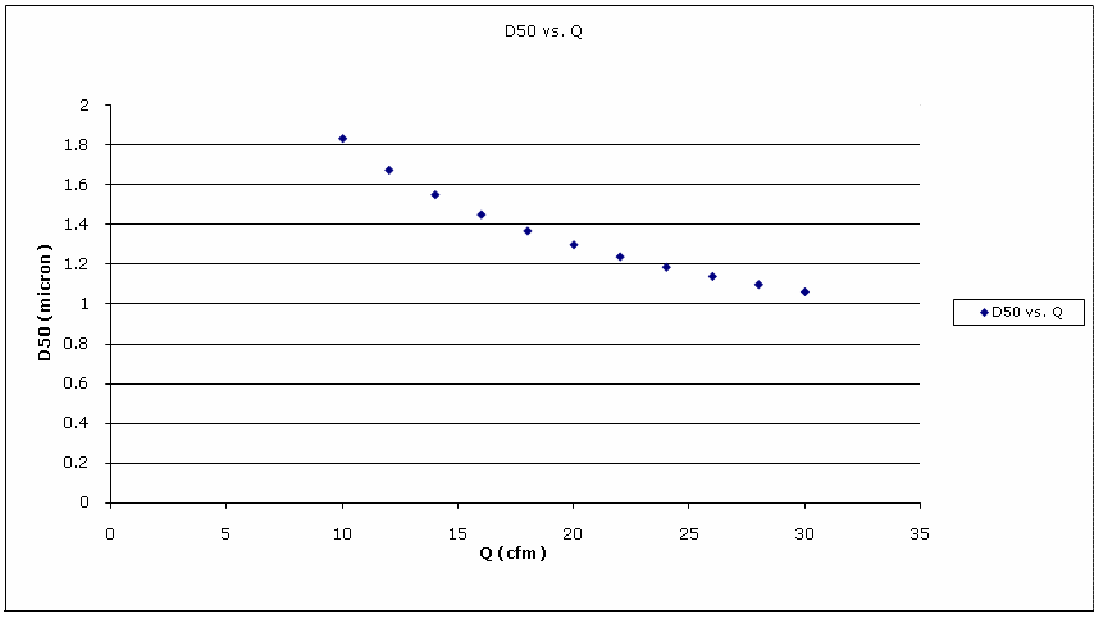

Figure [2.3.1]: d50 vs. flow rate Q

Theodore and DePaola [10] provide a prescription for calculation of the overall cyclone efficiency *e* over a range of aerodynamic particle diameters, d_i.

$$e_i = \frac{1}{1+(d_{50}/d_i)^2} \qquad \text{(Eq. 3)}$$

The calculated efficiency curve for our cyclone is shown in Figure [2.3.2].

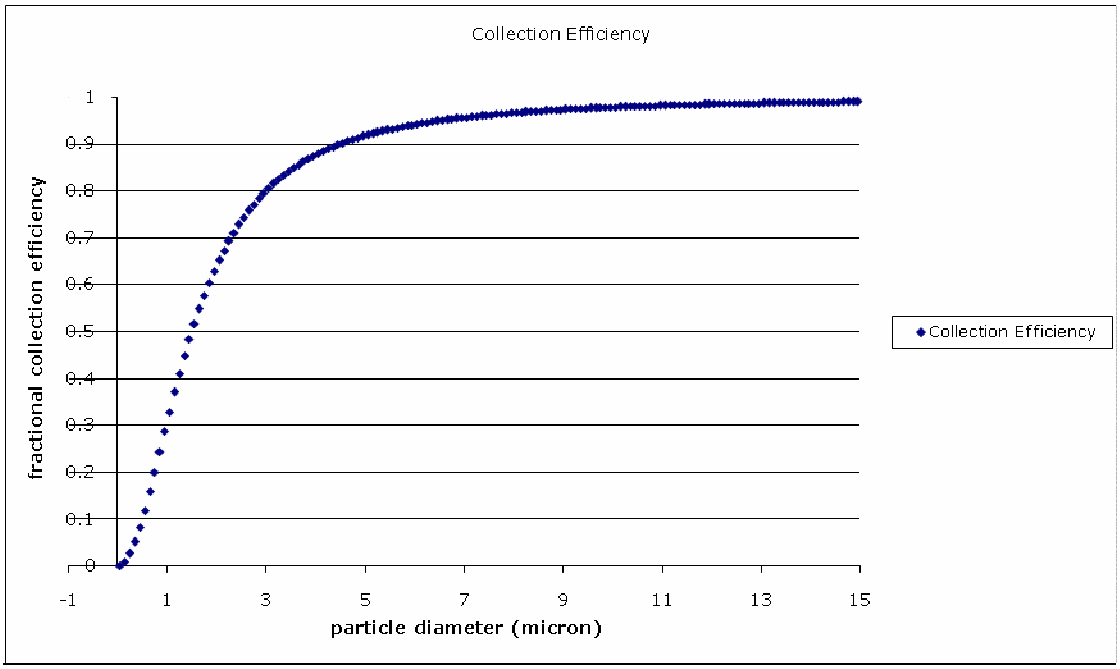

Figure [2.3.2]: Fractional Collection Efficiency vs. Aerodynamic Particle Diameter

As is apparent from Figure [2.3.2], we should expect to filter particles of diameter 4.5 microns at about the 90% level, with increasing collection efficiency for particles larger than 4.5 microns.

3.0 Equipment Description

3.1 Experimental Components

The apparatus for the experiment is broken down into sections and will be explained in further detail in the following subsections.

3.1.1 HEPA Filters F1 and F2

Filters F1 and F2 were HEPA compliant compressed air filters that trap particulates down to 0.01 micron. The filter housing is die cast aluminum. A large total

filtration area allows these filters to operate at 64 cfm with a pressure drop of only about 0.1 psi.

Figure [3.1.1]: Filters F1 and F2

3.1.2 Oilless Regenerative Blower

The air pump for the experiment was a 1/8 HP regenerative blower capable of pulling 27 cfm at a maximum working water pressure of 28" (1.0 psi). The blower was able to be mounted on any plane and was completely sealed against air leakage. 1.0" I.D. FPT inlets and outlets were used to interface with the tubing. Please see Table [3.1.1] for specifications.

Figure [3.1.2]: Oilless Regenerative Blower

Horsepower	1/8
Cubic Feet per Minute	27
Amperage Rating	2.0 continuous / 8.5 starting
Height (Decimal Inch)	8.5500"
Length (Decimal Inch)	8.7000"
Width (Decimal Inch)	7.7800"
Maximum Working Water Pressure (Decimal Inch)	28.5000"
Maximum Vacuum Water Pressure (Decimal Inch)	26.5000"
Voltage	115/230-1
Weight (lb)	16

Table [3.1.1]: Oilless Regenerative Blower Specs

3.1.3 Fluidizing chamber

The fluidizing chamber consisted of a 4” diameter, 36” long PVC pipe lined with metallic film to prevent the buildup of static charge, with an inlet coming in from the side at a 45 degree angle and an outlet on the top. The dust stimulant sat in the bottom, and as the air flowed in, it would fluidize the dust and would leave through the outlet. End caps were fitted with an attachment on the top end for 1.0” I.D. hose inlet and outlet. The chamber was loaded with sufficient simulant for several hours of operation. To maintain cabin air quality, the chamber was sealed at all times during flight.

Figure [3.1.3]: Fluidizing chamber

3.1.4 Inertial Separator (Cyclone)

Our cyclone unit was custom manufactured to the specifications of the experiment by RSG, Inc. The cyclone was optimized for flow rates of 10-15 cfm with a *d50* near 2.0 microns. The unit was constructed of 304SS steel and had a 1.0" O.D. tangential inlet, and a 1.0" O.D. axial outlet. Particulate collection at the bottom of the unit was accomplished by attaching a custom-built PVC collection cup to the 1.0" O.D. dust outlet. Between the dust outlet and the dust collection cup there was a valve to prevent any dust from moving up during non-operation. The attachments were made by hose clamp to *Tygon* tubing inserted over a hose barb adaptor on the collection pot. The pot was emptied through a viton-sealed cap at the base of the pot. There was no need to empty the pot during the flight. All simulant removal took place on the ground through a HEPA filtered vacuum.

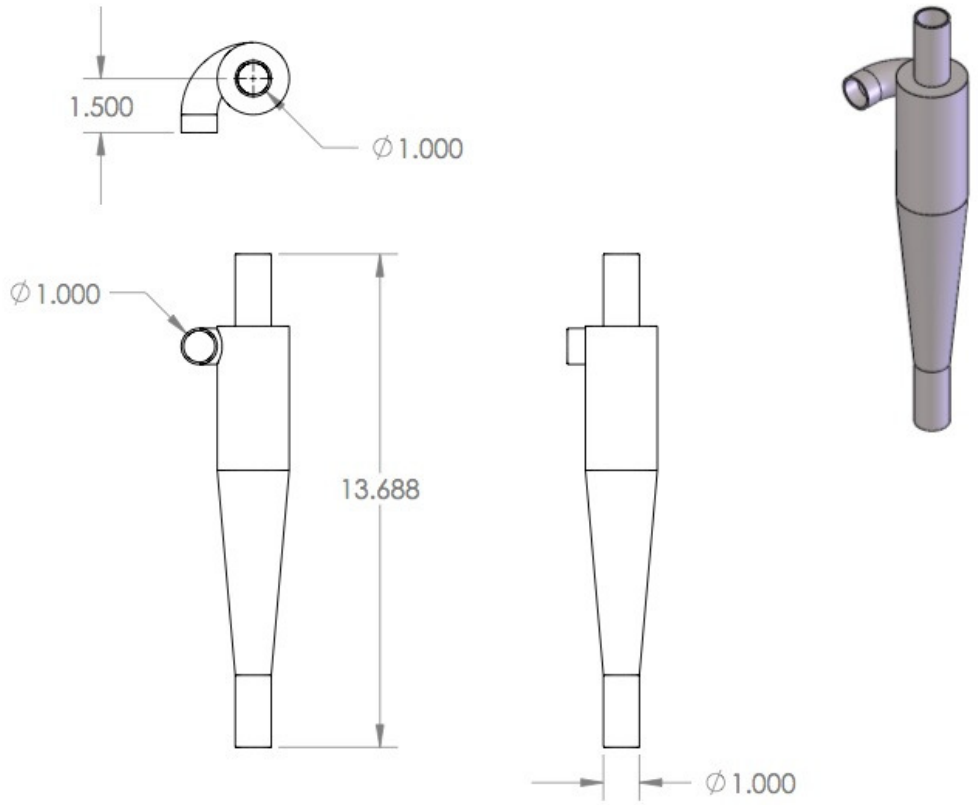

Figure [3.1.4]: Cyclone with tangential inlet and axial outlet. Dimensions are in inches.

3.1.5 Optical Particle Detectors (OPD)

Our team used three particle detectors. The first two were Lighthouse Handheld 3016 IAQ laser particle detectors on loan from Dr. Juan Agui at NASA-Glenn and Lighthouse Worldwide Solutions. The units permitted simultaneous measurement of six channels of particle sizes from 0.3 to 10.0 micron. The units had a self-contained pump operating at 0.1 cfm, and operated on a built-in Li-Ion battery. The particle detector was used to measure the amount of dust entering and leaving the cyclone. The third particle detector was an AM510 personal aerosol monitor. It was attached inside the flight rig but was not be part of the experiment. This detector was used to find any leaks in the experiment, to prevent any hazards from occurring.

Figure [3.1.5]: Lighthouse Handheld 3016 IAQ

3.1.6 Flow Valves and Flow Lines

Valves V1, V4, and V5 were panel-mounted, manually operated needle valves (steel construction) that were mounted on a 1/4" aluminum panel for operational access. Valves V2, V3, and V6 were smaller ball valves. V2 and V3 were for quickly opening and closing flow to the OPD units. Valve V5 was used in the event of a leak, to prevent any flow of the dust simulant. Valve V6 was used to cut off the dust collection pot from the rest of the system. This was closed off when the system was not in use and prevented the dust from moving up through the cyclone when the plane began to move into microgravity.

All flow lines utilized flexible, conducting plastic tubing. The flow through the OPDs was via 1/2" diameter tubing fitted to the isokinetic probe on the OPD. The rest of the flow lines utilized 1.0" I.D. tubing to minimize pressure drops in the circuit.

Two Y-connectors were fitted into the flow line, one before and one after the cyclone, to tap into the line for flow sampling to come as close to isokinetic sampling as possible. Isokinetic means that the air is flowing through the sample tube and the main line at the same speed. In Figure [3.1.6], (a) shows an example of ideal isokinetic

sampling. In that case, the particles in the air stream and the particles going into the sampling probe are traveling at the same speed. This setup allows for the most accurate reading.

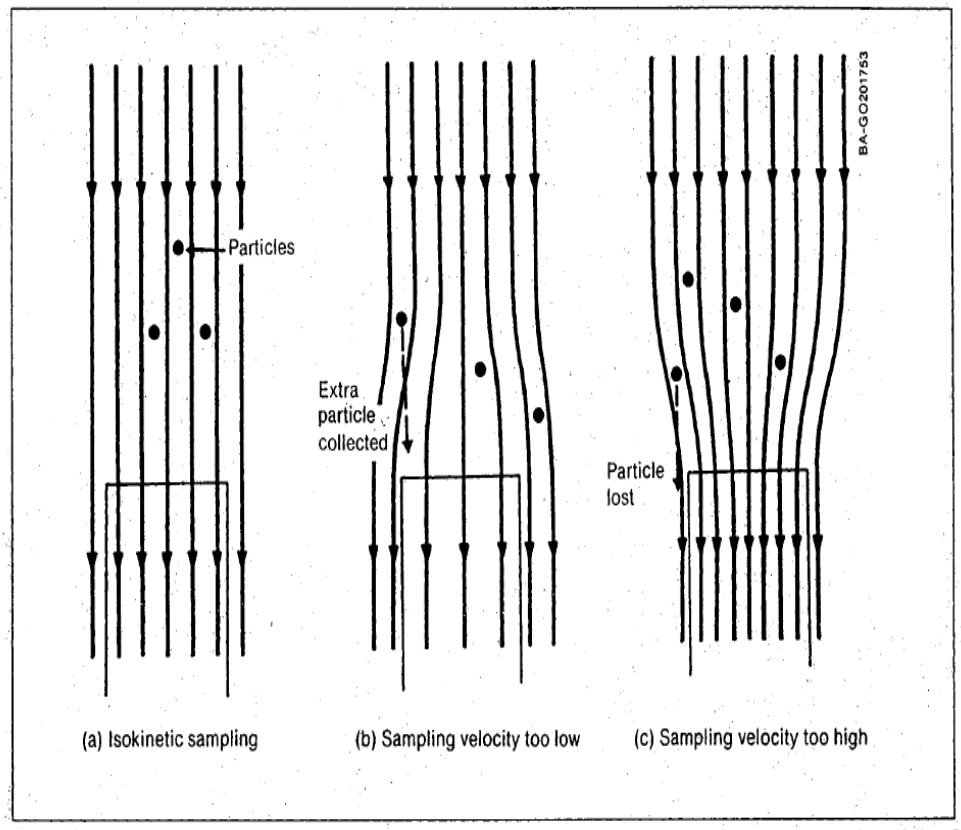

Fig. 7-10. Gas stream lines at the entrance to sampling probes (Source: Adapted from Strauss 1975, Fig. 2.12. © 1975. Used with permission of Pergamon Press)

Figure [3.1.6]: Gas stream lines at the entrance to sampling probes

In our case, this was not possible, and the closest we could get was using the Y-connectors. This caused the larger particles to get caught up at the bend and the smaller particles to move faster into the tube, not only because of the bend, but also because the tubing going to the particle detector was 1/2" and the main line was 1".

In our experiment, because of the pressure drop across the cyclone, there was less pressure in the system post cyclone. The pump in the OPD was unable to adjust for that,

and was able to pull air from the system much easier. Therefore, post cyclone, the OPD was able to test a larger amount of air.

3.1.7 Valve Plates

Two of the valve plates were bolted to the accessible long side of the flight rig, while the third was bolted across the top. They allowed for easy access to the six valves during the experiment when in reduced gravity. The three valve plates can be seen in Section 3.2, Figures [3.2.1] and [3.2.2].

3.1.8 Structural Components, Fasteners, and Flight Rig

Three-eighths inch U-bolts were used to attach the components to the vertical base plate of the flight rig. The vertical base plate was attached to the back of the flight rig as described below. The two filters, the cyclone, and the fluidizing chamber will be attached to the aluminum vertical base plate during the flight.

The blower was bolted to a shelf, built into the flight rig. The shelf stayed in place by bolting it to the rig, using a Support Beam on one side and a direct bolted attachment to the vertical base plate on the back edge of the shelf. The power strip was attached to the shelf using U-bolts.

The OPDs were attached to the top of the rig using Velcro, the valves were mounted to a valve plate, and all other components were bolted to a vertical base plate on the rig as shown in Figure [3.2.1].

The bottom base plate was part of the flight rig, and was included in the structural analysis of the rig. The base plate has 1” bolt holes at a center-to-center spacing of 20” that matches the bolt pattern on the DC-9 floor.

3.2 Equipment Layout

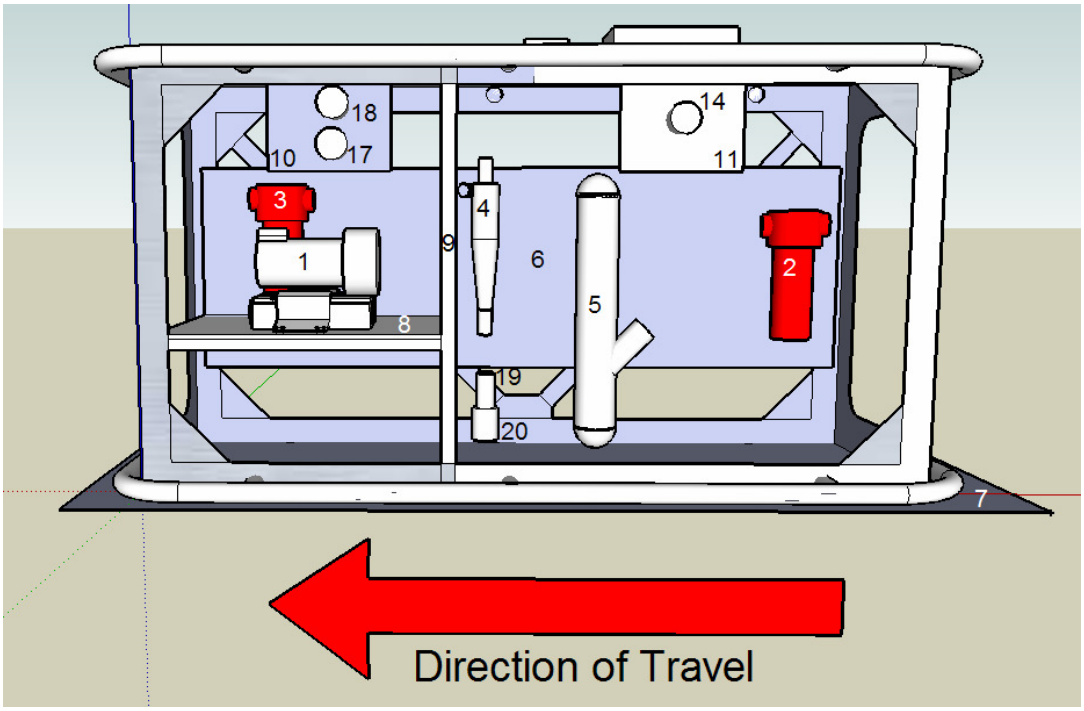

Figure [3.2.1]: Experimental Layout Diagram (Tubing and Fasteners not shown)

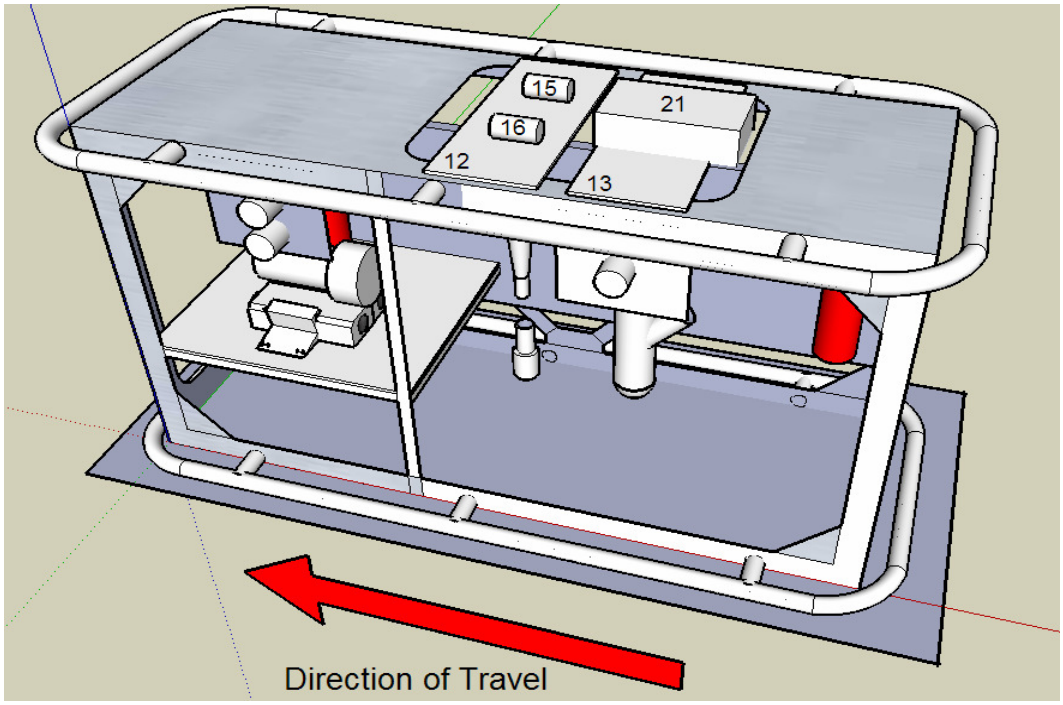

Figure [3.2.2]: Experimental Layout Diagram (Tubing and Fasteners not shown)

1. Blower
2. F1 HEPA Filter
3. F2 HEPA Filter
4. Cyclone
5. Fluidizing Chamber
6. Back Aluminum Plate
7. Base Plate
8. Shelf
9. Shelf Support Beam
10. Valve Plate 1
11. Valve Plate 2
12. Valve Plate 3
13. OPD Plate
14. V1
15. V2
16. V3
17. V4
18. V5
19. V6
20. Dust Collection Cup
21. OPD

4.0 Experimental Procedures

The first step in the procedure was to prepare the rig. To do this, we first made sure that the OPDs were shut off. Valves V1 and V3 were closed and valves V2, V4, V5, and V6 were all opened all the way. Next, the blower was turned on and allowed to run

for about 30 seconds. Then, the OPDs were turned on; OPD1 was set to 'Pre-Lune' mode and OPD3 was set to 'Post-Lune' mode. After each of the OPDs were set up to take 20 seconds of data, the rig was ready to begin testing.

For the ground tests, after the rig was prepared to start, the start button was pressed on each of the OPDs and they would automatically stop after the 20 seconds of testing. The results of these tests were stored on each respective OPD and once all of the tests were done, those results were ported to the computer were they could be analyzed.

For the reduced gravity experiments, as soon as the lunar or Martian gravity was reached, the start buttons on each OPD were pressed at the same time, and again the OPDs would stop testing after the 20 seconds. This process was repeated for each of the reduced gravity parabolas. After the flight, the data was ported over to the computer were the results could be analyzed.

5.0 Results

Figure [4.1] shows the 1-g and 1/6-g results along with the calculated collection efficiency of the cyclone used in this experiment. The collection efficiency of the cyclone was calculated using an empirical model based on the *d50* cut number. The efficiency was determined by taking the difference between the pre and post cyclone counts and then dividing by the pre cyclone count to get a fractional difference (see Eq. 4).

$$e_i = \frac{N_{pre} - N_{post}}{N_{pre}} \qquad \text{(Eq. 4)}$$

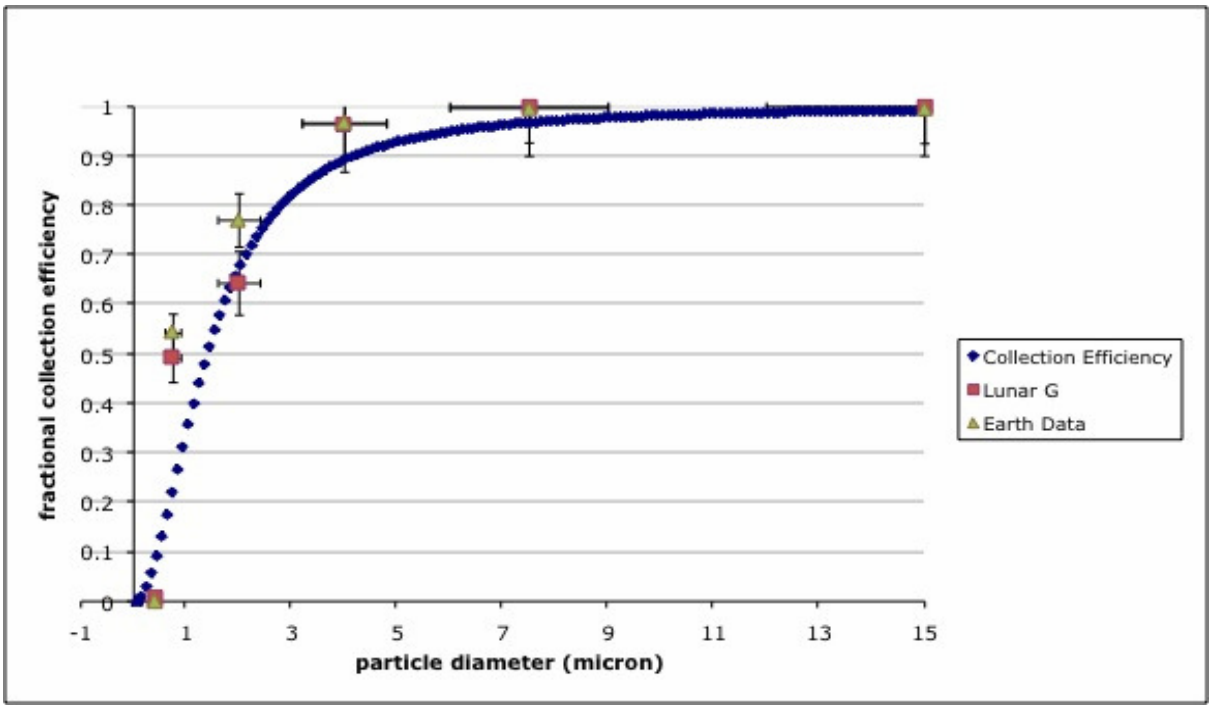

Figure [4.1]: 1-g and 1/6-g results

The collection efficiency shown in Figure [4.1] is based on an entirely empirical model. Therefore, we did not expect to have our data points follow the calculated efficiency as closely as they did.

The standard deviation in the x-direction was determined by the bin sized of the OPDs. The standard deviation in the y-direction was determined by determining the efficiency of each individual 20 second test for each bin, taking the average, and then putting it into Equation 5, where *SD* is the standard deviation.

$$SD = \frac{\sqrt{\sum_i (avg - e_i)}}{i - 1}$$

(Eq. 4)

The results show that at larger diameters, the cyclone is almost 100% as efficient in lunar gravity as it is in earth gravity. As the particle sizes get smaller, the efficiency

goes down for lunar gravity more so than earth gravity, although this difference is within, or close to, a standard deviation for all particle sizes except 2.0 microns, where there is a 2 standard deviation difference.

.

6.0 Discussion

We have shown through this experiment that the cyclone does work in reduced gravity environments, although there does seem to be a gravitational effect on efficiency. We expected to see a difference caused by a slower flow rate due to a drop in pressure while at altitude, but while onboard the plane, a flow meter was used to test the flow rate at the outlet and this was not the case. We found no difference in the flow rate between ground tests and flight tests.

Another problem that was encountered was a pressure drop over the cyclone. This pressure drop caused a change in the flow rate which would affect the particle counts. The particle detectors were unable to compensate for that difference. To compensate for the difference in counts caused by the pressure drop, we need to better understand how that change is affecting our counts and determine a way to mathematically account for the differences.

Another source of error in this experiment was that two different particle detectors were being used. When testing them on the ground against each other, there were differences in the counts of the larger sized particles. Using ground test data, we were able to calibrate the two OPDs against each other to account for that difference.

The results of this experiment suggest that a cyclone could be a feasible choice for the first stage in a multi-stage filtering process for future lunar and Martian habitats. It

also shows the need for more testing of inertial filtration systems in reduced gravity environments to fully understand the effect of reduced gravity on efficiency.

7.0 Bibliography

1. Flinn, E. D. Solving Settlement Problems: Dealing with Moon Dust. *Space.com.* Retrieved January 19, 2008, from http://www.space.com/adastra/adastra_moondust_060223.html

2. Rincon, P. Lunar Dust 'May Harm Astronauts' *HealthNews 24/7.* Retrieved January 24, 2008, from http://healthnews247.com/health-news-today/Lunar-dust-may-harm-astronauts/

3. Roy, S. Unique NASA Science Lab Tackles 'Sticky' Issue of Lunar Dust. *NASA.* Retrieved January 19, 2008, from http://www.nasa.gov/centers/marshall/news/news/releases/2005/05-144.html

4. Bell, T. E. Lunar Dust Buster. *NASA.* Retrieved January 19, 2008, from http://science.nasa.gov/headlines/y2006/19apr_dustbuster.htm

5. Phyllips, T. The Smell of Moondust. *Science@NASA.* Retrieved January 19, 2008, from http://science.nasa.gov/headlines/y2006/30jan_smellofmoondust.htm

6. Gilmour, M. I., Daniels, M., McCrillis, R. C., Winsett, D., & Selgrade, M. K. Air Pollutant-Enhanced Respiratory Disease in Experimental Animals. *Environ Health Perspect*, *109*(4), 619-622. August 2001

7. Shepherd, C. B., and Lapple C. E. Flow Pattern and Pressure Drop in Cyclone Dust Collectors. Industrial and Engineering Chemistry. 31(8): 972-984, 1939

8. Longe, J. L. "Silicosis." Encyclopedia of Medicine. 19 Jan. 2008, from http://www.enotes.com/medicine-encyclopedia/silicosis

9. Asaravala, A. What a Little Moon Dust Can Do. *Wired.* Retrieved January 19, 2008, from http://www.wired.com/science/space/news/2005/04/67110

10. Theodore, L. and DePaola, V., "Predicting Cyclone Efficiency," Journal of the Air Pollution Control Associate, Vol. 30, No. 10, 1980.